BioSystems 130 (2015) 1–10

Contents lists available at ScienceDirect

BioSystems

journal homepage: www.elsevier.com/locate/biosystems

Review

Mathematical modelling of fluid transport and its regulation at multiple scales

Osvaldo Chara [a,b], Lutz Brusch [b,*]

[a] Institute of Physics of Liquids and Biological Systems (IFLYSIB), National Scientific and Technical Research Council (CONICET) and National University of La Plata (UNLP), Calle 59 No. 789 (1900), La Plata, Argentina
[b] Center for Information Services and High Performance Computing, Technische Universität Dresden, Dresden 01069, Germany

ARTICLE INFO

Article history:
Received 10 July 2014
Received in revised form 4 February 2015
Accepted 4 February 2015
Available online 7 February 2015

Keywords:
Osmosis
Cell volume homeostasis
Cyst lumen
Mathematical model

ABSTRACT

Living matter equals water, to a first approximation, and water transport across barriers such as membranes and epithelia is vital. Water serves two competing functions. On the one hand, it is the fundamental solvent enabling random mobility of solutes and therefore biochemical reactions and intracellular signal propagation. Homeostasis of the intracellular water volume is required such that messenger concentration encodes the stimulus and not inverse volume fluctuations. On the other hand, water flow is needed for transport of solutes to and away from cells in a directed manner, threatening volume homeostasis and signal transduction fidelity of cells. Feedback regulation of fluid transport reconciles these competing objectives. The regulatory mechanisms often span across multiple spatial scales from cellular interactions up to the architecture of organs. Open questions relate to the dependency of water fluxes and steady state volumes on control parameters and stimuli. We here review selected mathematical models of feedback regulation of fluid transport at the cell scale and identify a general "core–shell" structure of such models. We propose that fluid transport models at other spatial scales can be constructed in a generalised core–shell framework, in which the core accounts for the biophysical effects of fluid transport whilst the shell reflects the regulatory mechanisms. We demonstrate the applicability of this framework for tissue lumen growth and suggest future experiments in zebrafish to test lumen size regulation mechanisms.

Contents

* Corresponding author. +49 35146338553.
E-mail address: lutz.brusch@tu-dresden.de (L. Brusch).

http://dx.doi.org/10.1016/j.biosystems.2015.02.004
0303-2647/

1. Introduction

Water is the dominant component of living cells and therewith organisms constituting around 70% by mass and 98% by molecule number of an animal cell (Freitas, 1999). Certifying the essential role of water, it features prominently in theories for the origin of life (Ganti, 2003). Regardless of which aspect of life emerged first, all come with an inherent requirement for transport of matter at the molecular scale. Water as a solvent had fulfilled this requirement already in prebiotic chemical systems. Chemistry also calls for the right amount of thermal fluctuations in a life-supportive temperature range. But as everything, the aqueous chemical system is subject to the laws of thermodynamics which render the spontaneous generation of more complex molecules extremely rare (Landau and Lifshitz, 1980).

One of Gánti's principles of life is therefore the existence of a transport barrier as a system boundary (Ganti, 2003). In the thermodynamic picture, system boundaries allow a system to stay out of the thermodynamic equilibrium, to dissipate energy and increase the degree of order within the system (Busse and Müller, 1998). Different forms of barriers around living systems have evolved including membranes around cells and epithelial tissue sheets around organs. Biological membranes self-assemble due to the hydrophobic effect induced by the hydrogen-bond network – based on the water structure (Ferrara et al., 2012) and the hydrophobicity of the lipid tails which reciprocally establish an intrinsic water barrier.

On the other hand, life requires exchange across the barrier and, correspondingly, tightly regulated transport mechanisms have evolved at the different scales. Cells possess specific and regulated channels to control transport across the cell membrane and organelle membranes. Epithelial cells are polarised apical versus baso-lateral enforcing directionality of transport at higher scales.

We here focus on mathematical models of fluid transport across barriers at the cellular and the tissue scale and its regulation which links multiple spatial scales. This review starts by outlining a bigger picture of multi-scale feedback regulation and then compares selected mathematical models of feedback regulation of fluid transport at the cell scale to identify a general "core–shell" structure of such models. We then analyse models of tissue lumen growth from the core–shell perspective. We propose model extensions by incorporating feedback regulation *via* processes at different scales, list related open biological questions and conclude.

2. A need for multi-scale feedback regulation

Water is the fundamental solvent and facilitates the passive diffusion of molecular compounds and therewith the biochemistry of metabolic pathways. In metabolism, any given carbon atom has to visit a number of subsequent enzymes and hence the molecules have to be mobile. The law of mass action for chemical reactions relates the substrate concentrations *via* the probability of random encounters between substrate (and enzyme and cofactor) molecules in the solution to the reaction flux. When $N(t)$ is the number of substrate molecules and $V(t)$ the volume of the compartment, *e.g.* the cell, then the concentration $c(t) = \frac{N(t)}{V(t)}$ may change upon volume changes, that is, due to changing osmotic conditions. Hence, metabolite and signal transducer concentrations reflect both, pathway activation targeting $N(t)$ and inverse volume changes $\frac{1}{V(t)}$. The effects of the volume dependence are amplified when multiple components take part in a reaction, *e.g.* the enzyme, multiple substrate molecules, cofactors like ATP and NADH as well as allosteric activators. Then all their concentrations change as $\frac{1}{V(t)}$ in synch and the reaction flux changes with a high power of $V(t)$. To account for such potentially far-reaching effects in mathematical models, volume changes have to become an explicit model component.

Within such a variable cell volume modelling framework, the equation governing the cellular concentration $c(t)$ as function of time is

$$\frac{dc}{dt} = \frac{d\frac{N(t)}{V(t)}}{dt} = \frac{1}{V}\frac{dN}{dt} + \frac{N1}{VV}\left(-\frac{dV}{dt}\right) \quad (1)$$

where the right hand side combines the effects of the biochemistry (first term) and those of the biophysics, the second term with the dilution rate $\frac{1}{V}\left(-\frac{dV}{dt}\right)$.This general equation particularly applies to metabolite concentrations within growing or otherwise changing cells (Maria, 2005, 2014). On larger scales, embryonic organogenesis in many cases passes an epithelial cyst state as highlighted by in vitro organoid self-organisation of mini-guts (Sato and Clevers, 2013), optic cups (Eiraku et al., 2011), mini-brains (Lancaster et al., 2013) and other structures from embryonic stem cells (Bedzhov and Zernicka-Goetz, 2014). It has been proposed that "luminal signalling provides a potentially general mechanism to locally restrict, coordinate and enhance cell communication within tissues" (Durdu et al., 2014). As recently quantified for secreted FGF ligands within the microlumen of tissue rosettes, luminal ligand concentration controls organ formation (Durdu et al., 2014). These rosettes of the zebrafish lateral line primordium eventually form mechanosensory organs and to work correctly, lumen formation ($V(t)$) has to be coordinated with ligand secretion ($N(t)$).

In all these cases at different scales, changes in $V(t)$ could be substantial and non-monotonic since water is also the medium that transports solutes to and away from cells. This second and competing role of water requires especially secretory gland cells to replenish water outside of their apical membranes by allowing water efflux. The amount of water efflux has to fulfil a variable demand at the higher tissue scale which then threatens to compromise cell volume homeostasis and signal transduction fidelity, relying on $c \sim N$. Moreover, the hydrostatic pressure of water within a closed compartment is a driving force for tissue morphogenesis, especially for cyst expansion and tubulogenesis. Again, the tissue scale morphogenetic demands entail cellular water efflux and threaten cell volume homeostasis. To rescue cell volume homeostasis despite variable water efflux, regulatory feedback loops are needed and might have to span multiple spatial scales.

The general principle of multi-scale feedback loops is illustrated in Fig. 1 where the spatial scale increases from left (a) to right (c). Fundamental biophysical interactions propagate effects from lower to higher scales (denoted by dashed arrows) while regulatory interactions propagate effects from higher to lower scales (solid arrows in Fig. 1). Jointly, these interactions form multiple feedback loops spanning across all spatial scales. These multi-scale feedback loops reconcile two competing roles of water

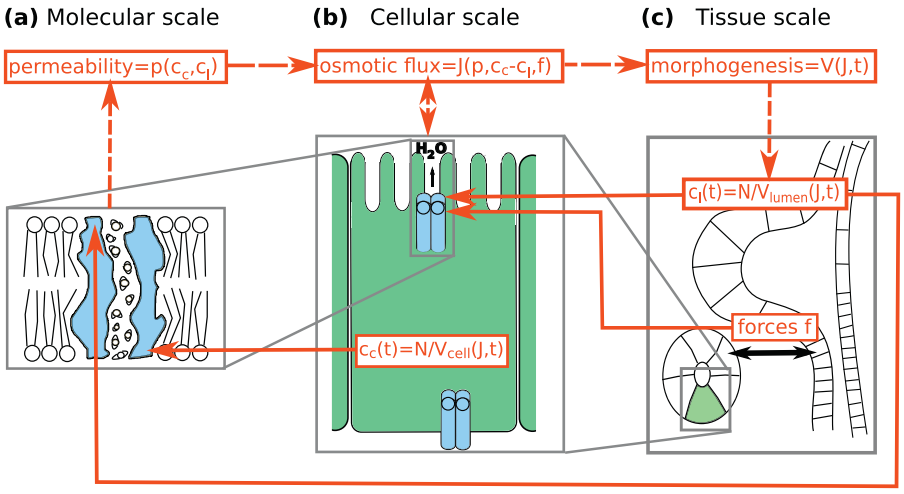

Fig. 1. Multi-scale feedback regulation of water transport. Dashed arrows denote the dependence of emergent properties (red boxes) at higher scales on variables at lower scales. Solid arrows denote the regulation of variables at lower scales by properties at higher scales. Jointly, these interactions form multiple feedback loops spanning across all spatial scales. (a) The molecular structure and density of water channels (here sketched together with a portion of the lipid bilayer) as well as regulatory molecule concentrations inside the cell (c_C) and outside the cell, in the lumen (c_l), control the water permeability (p) of membranes. (b) At the cellular scale, cell volume (V_{cell}) is changed by water flux (J) and affects the concentration of intracellular regulators (c_C). The osmotic water flux (red box on top) depends on molecular scale variables (p), on cellular scale variables (apical surface area and c_C) and on tissue scale variables (f and c_l). (c) Tissue morphogenesis and function depend on water fluxes (J) which change lumen volumes and concomitantly pressures and forces (f) between tissues (here, two perpendicular elastic ducts are sketched). Extracellular regulators are diluted (c_l) by increasing lumen volume. (For interpretation of the references to colour in this figure legend, the reader is referred to the web version of this article.)

for life, as a solvent on the one hand and as a transport infrastructure on the other hand.

An illustrating example of the multi-scale regulation of fluid transport is given by the enterohepatic circulation of bile salts (Kubitz and Häussinger, 2007). Bile salts are required in the small intestine to help in the digestion of fatty nutrients. In order to reduce the need for *de novo* synthesis of bile salts, the enterohepatic circulation recycles bile salts with a quota of 95%. In brief, bile salts are absorbed from the ileum and venous blood delivers them through the hepatic portal vein and liver sinusoids to hepatocytes, which clear the bile acids from the blood very efficiently such that little leaks into the systemic blood circulation of the body.

On the return route for bile salts from hepatocytes *via* the gall bladder to the duodenum, there is no blood system helping and hepatocytes also have to secrete the water for transporting the bile acids. By means of proteins called BSEP, for bile salt export pump, bile acids are pumped from the hepatic cytoplasm into the lumen, called bile canaliculus, which is enclosed by apical membrane of adjacent hepatocytes. The bile acid concentration gradient drives an osmotic water flux from hepatocytes into the lumen which transports the bile acids *via* bile ducts to the gall bladder (Kubitz and Häussinger, 2007). In turn, hepatocytes themselves have to take up water from the blood. The hepatocyte has evolved control loops of osmotic balance to maintain volume homeostasis despite a significant water flux through each cell (Mühlfeld et al., 2012). This need for tight regulation has already attracted many mathematical modelling studies on hepatocytes and other cell types (Chara et al., 2009, 2010; Pafundo et al., 2008; Schaber and Klipp, 2008; Klipp et al., 2005).

Thanks to the nontrivial homeostasis of cell volume for many cell types, as presented in Section 3, the concentrations instead of particle numbers of solutes can function as signals that are transduced from receptors to distant effectors without deteriorating their message due to otherwise fluctuating dilution in case of random volume variations. Moreover, the commonly used implicit assumption of constant cell volume when deriving ordinary differential equation models of metabolism can be justified in many conditions.

3. Cellular scale aspects

3.1. Fluid transport and cell volume homeostasis

In order to produce body fluids, cells secrete water and solutes across their membranes potentially at the expense of their cell volume. Maintenance of cell volume in the face of fluctuating intra- and extra-cellular osmolarity is essential for cell function. In contrast to plant cells, animal cells cannot withstand osmotic gradients across their membranes. Therefore evolution led animal cells to develop mechanisms capable of sensing and adjusting osmolarity to control cell volume, for the well-understood case in yeast (Schaber and Klipp, 2008; Klipp et al., 2005). More generally, there are two main mechanisms for cell volume regulation according to the time scale involved (Fig. 2a): long-term and short-term (Baumgarten and Feher, 1995; Hallows and Knauf, 1994). The long-term cell volume regulation is due to the activity of the Na^+ pump (Baumgarten and Feher, 1995; Byrne and Schultz, 1988; MacKnight, 1987). This pump counterbalances the passive cell tendency to slowly gain cations followed by water until the Gibbs–Donnan equilibrium is reached. We briefly summarise the regulatory mechanisms for cellular volume homeostasis, then review the mathematical models for one class of these mechanisms, namely short-term cell volume regulation mediated by electrolytic solutes, to deduce a common core–shell framework.

The short-term cell volume regulation can be made evident by exposing cells to an external medium with different osmolarity than the one of the cytosol. When cells are exposed to external hypotonicity, the generated osmotic gradient across the plasma membrane causes water influx and cell swelling. However, during continuous hypoosmotic stress, cells undergo a slower secondary shrinkage. This response is known as regulatory volume decrease (RVD) mechanism, which prevents cell disruption, maintaining cell viability. RVD is mediated to a large extent by a net efflux of osmotically active solutes mainly through the swelling-activated K^+ and Cl^- channels (Jakab et al., 2002; Lang et al., 1998). A rapid water efflux is osmotically triggered mainly through aquaporins which are coupled to the channels. For instance, AQP2 is functionally linked to Cl^- (the cystic fibrosis transmembrane

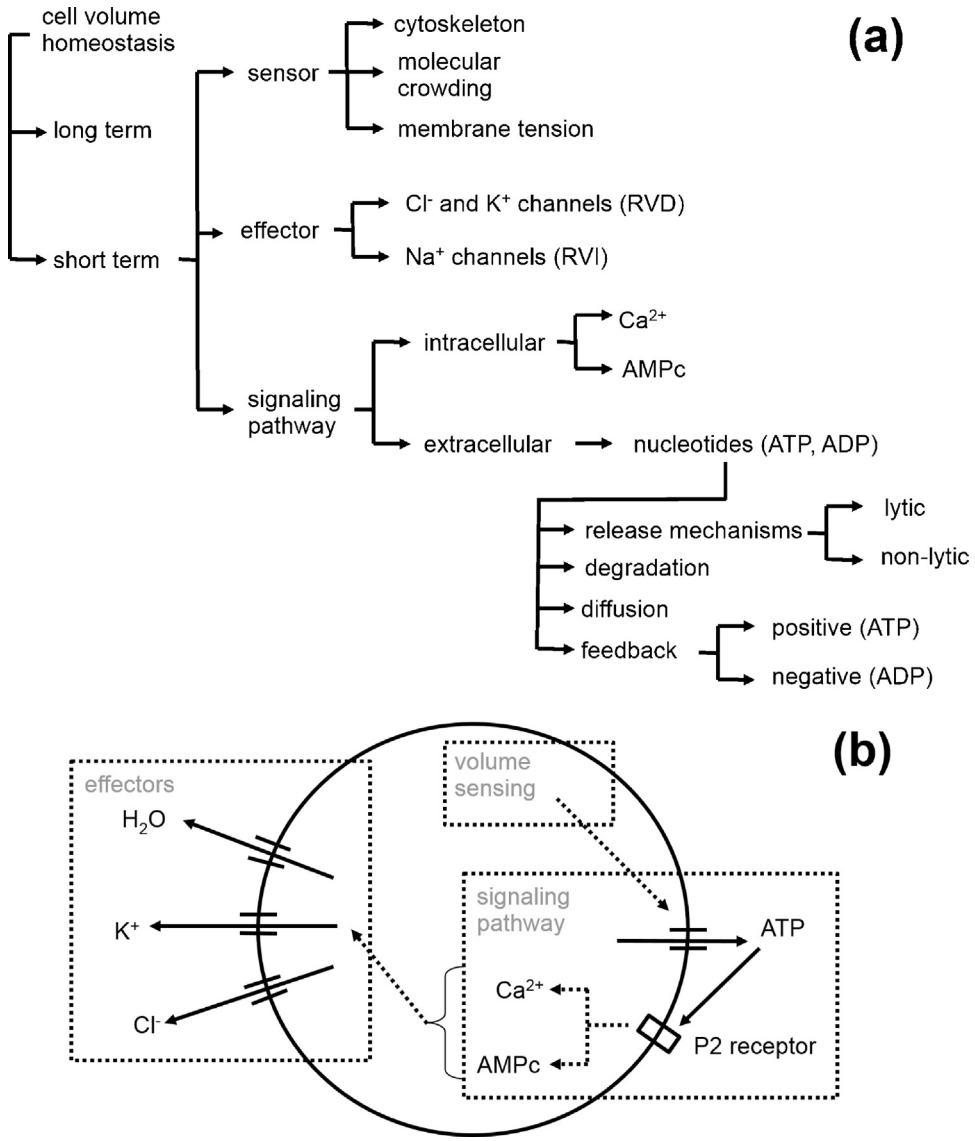

Fig. 2. Cell volume regulation elements. (a) Main characteristics of cell volume regulation. (b) Scheme showing the interrelation among the different elements responsible for cell volume regulation.

conductance regulator, CFTR) and to K^+ channels (Ford et al., 2005). Similarly, exposition to hypertonicity causes cell shrinking which is followed by a volume increase, the so-called regulatory volume increase (RVI) mechanism. This process is due to an influx of solutes which involves transporters like the Na^+/H^+ exchanger NHE1 and the Na^+, K^+, $2Cl^-$ cotransporter NKCC1. In addition to these proteins, other effectors can be found in RVD and RVI (Hoffmann et al., 2009; Lang et al., 1998).

There is a growing body of evidence showing that extracellular nucleotides, mainly ATP, play an important role as extracellular signals in cell volume regulation. This nucleotide is released under hypotonic exposition to the extracellular medium where it binds to P receptors in the cell membrane (Lazarowski et al., 2003) which activate K^+ channels (the effector mechanism) and, consequently, yields RVD in almost the entire animal kingdom (for reviews see (Hoffmann et al., 2009; Lang et al., 1998), for vertebrates or (Chara et al., 2011), specifically for fish, and references therein). Thus, ATP modulates RVD through autocrine and paracrine mechanisms (Wang et al., 1996).

3.2. Modelling fluid transport at the cell level: short-term cell volume regulation

Cell volume is rather flexible since there are sufficient intracellular membrane and extracellular water to increase it easily. As pointed out above, cell volume inversely determines all molecular concentrations and thereby affects the allosterically regulated enzyme activities with undesirable effects. Cell volume homeostasis is hence of central importance to life. In general, mathematical models of short-term cell volume regulation include water as well as solute transport processes. Essentially, the mathematical models conceived so far follow the Kedem–Katchalsky formalism (Kedem and Katchalsky, 1958). This formalism is based on the thermodynamics of irreversible processes. Briefly, the models assume that all the molecular entities (solutes and solvents) are subject to fluxes which are functions of driving forces.

Electrolytic solute transport can be modelled as an electro-diffusive process (described by the Goldman–Hodgkin–Katz

equation, see Section 3.2.2) coupled with a cell volume regulation mechanism. Using a descriptive image, the underlying model equations can be understood as the "core" and the "shell" of the model, respectively, where the core covers the fluid and solute transport whilst the shell reflects the regulatory fine-tuning mechanism. The shell can be characterized by three elements (Altamirano et al., 1998): a volume sensor, an effector and a signalling process coupling them (Fig. 2a and b).

3.2.1. The "core" of modelling fluid transport at cellular level: water transport

Water transport across a membrane has been described in many models using the phenomenological law of osmosis (Pickard, 2008; Landau and Lifshitz, 1980). Water flux (J_W, $cm^3\,s^{-1}$) is given by:

$$J_W = P_{OSM} A V_W \left(\frac{\sum_i m_i}{V} - C_e \right) \tag{2}$$

where A, V_W, P_{OSM}, m_i, V and C_e are the cell surface area available for water transport, partial molar volume for water (approx. 18 $cm^3\,mol^{-1}$), water osmotic permeability (in $cm\,s^{-1}$, representing the mean velocity across the considered area), the molecule number of intracellular solutes for species i, the cell volume and the extracellular concentration, respectively. Since cell volume is proportional to the water content, the continuity theorem states:

$$\frac{dV}{dt} = J_W \tag{3}$$

from which it can be readily concluded:

$$\frac{dV}{dt} = P_{OSM} A V_W \left(\frac{\sum_i m_i}{V} - C_e \right) \tag{4}$$

The previous consideration implicitly assumes that the reflection coefficient is close to one, which is reasonable for the majority of the relevant solutes under standard conditions (Chara et al., 2011).

3.2.2. The "core" of modelling fluid transport at cellular level: solute transport

Ion movements through membrane structures are usually modelled including their dependence on concentrations on both membrane faces and the electrical potential difference between both intracellular and extracellular compartments. The flux corresponding to the ion j can be described by:

$$J_j = P_j u \left(\frac{C_{ej} - \frac{m_j}{V} e^{-u}}{1 - e^{-u}} \right) \tag{5}$$

In this expression derived by Goldman (1943), modified by Hodgkin and Katz (1949), J_j (in $mol\,s^{-1}$) is the passive flux of the charged ion j, u is a normalized membrane potential (without units), P_j is the single ion permeability for ion j (in $cm\,s^{-1}$), whereas the difference between extra- (C_{ej}) and intracellular (m_j/V) concentrations of a given ion (in $mol\,cm^{-3}$) – weighted by a factor dependent on u – accounts for the electrochemical gradient. Finally, the normalized potential u is defined as $FV_m/(RT)$, with F being the Faraday constant (about 96,500 $C\,mol^{-1}$), V_m the membrane potential (in V), R the gas constant and T the absolute temperature (in K).

Around this "core" describing solute transport, a "shell" of cell volume regulation can be incorporated. The "shell" can include long-term cell volume regulation involving ion pump activities or short-term cell volume regulation processes reflecting mainly transporters. In the next sections, the latter processes are specifically addressed.

3.2.3. The "shell" of modelling fluid transport at cellular level: short-term cell volume regulation based on cell volume-dependent ion permeability

The control of cell volume was introduced for the first time in a mathematical model more than twenty years ago (Strieter et al., 1990). The model described cell volume changes in polarized cells forming a tight epithelium (polarised refers to cells having a non-homogeneous membrane; *i.e.* the cell shows apical and basolateral membranes which differ in area and channel content). The authors formalised an idea that originated in the Danish physiological community. They proposed that ion permeability could not be a constant but rather a function of the cell volume:

$$P_j = P_j^0 \left(1 + \frac{M_j}{1 + \exp(-\xi(V - V_{1/2}))} \right) \tag{6}$$

with P_j^0 the basal isotonic permeability of ion j, M_j the maximum factor by which permeability of ion j may increase, V the actual cell volume, $V_{1/2}$ the cell volume at which the change in permeability of ion j is half of its maximum value, and ξ the compliance (inverse of stiffness) of the basolateral membrane. Thus, the permeability of ion j is a sigmoidal function of cell volume which is compatible with a step like saturable activation of channels activated by mechanical forces acting during swelling: the so-called mechano-sensitive channels. Although the model was developed for cells suffering a hypotonic shock and, consequently, showing RVD, this strategy can be likewise used for RVI, replacing $(V - V_{1/2})$ by $(V_{1/2} - V)$. This function involving a cell volume-dependency of ion channels has already been successfully applied (Terashima et al., 2006; Novotny and Jakobsson, 1996).

3.2.4. The "shell" of modelling fluid transport at cellular level: short-term cell volume regulation based on cotransport of ions sensing cell volume and chemical gradients

Another strategy to model RVD and RVI was proposed almost ten years later (Hernandez and Cristina, 1998). The idea was to assume that solute and water transport follow the equations considered in Sections 3.2.1 and 3.2.2 if and only if the actual cell volume is lower than a critical cell volume, for the case of RVI, or higher than the critical value, for the case of RVD. Once the cell volume exceeds the critical value, a cotransport mechanism would be triggered. The authors assumed that RVD and RVI would be mediated by KCl efflux and NaCl influx which would be governed by the following expressions:

$$\phi_{KCl} = Q^*_{KCl} \left(\frac{V - v_{RVD}}{v_{RVD}} \right) \left(C_{eK^+} C_{eCl^-} - \frac{m_{K^+} m_{Cl^-}}{V^2} \right) \tag{7}$$

$$\phi_{NaCl} = 0 \tag{8}$$

for $V \geq v_{RVD}$

$$\phi_{NaCl} = Q^*_{NaCl} \left(\frac{v_{RVI} - V}{v_{RVI}} \right) \left(C_{eNa^+} C_{eCl^-} - \frac{m_{Na^+} m_{Cl^-}}{V^2} \right) \tag{9}$$

$$\phi_{KCl} = 0 \tag{10}$$

for $V \leq v_{RVI}$ where C_{ej} and m_j, are the external concentration and the number of intracellular moles of ion j. φ_j and Q_j^* represent the cotransported flux of the ion j and a parameter which represents the maximal flux of ion j to be cotransported, *i.e.* a sort of amplitude of cotransport. V, V_{RVD}, V_{RVI} are the actual cell volume and the critical ones under RVD and RVI, respectively. Furthermore, the RVD cotransport mechanism would be dormant whilst cell volume is lower than V_{RVD}. Once the cell volume exceeds this value, a cotransported efflux of KCl will be driven by the concentration

difference between both ends of cotransporters (between both plasma membrane sides) and weighted by a relative distance between actual volume and the critical one and tuned with the amplitude for potassium. Concurrently, the model assumes that cotransport of NaCl is null. Similarly, when cell volume would be lower than V_{RVI}, the RVD mechanism would become silent and the RVI would be turned on, given by the influx of NaCl whilst KCl efflux would then vanish. Additionally, the model assumes that there can be a time lag τ between the moment at which the difference between cell volume and a critical volume is evaluated in an indirect way and the response of the ion fluxes. The mentioned strategy was successfully corroborated after fitting to experimental results in hepatocytes from rat, trout, and goldfish (Espelt et al., 2008). Again, it is possible to identify the model elements underlying RVD or RVI. In this model it is possible to locate the volume sensor, the signalling process and the effectors in the parameters V_x (where x stands for RVD or RVI), τ and Q_j^*, respectively. While $V - V_x$ relates to the sensing of cell volume, the signalling process underlies the time lag parameter τ. The amplitude of cotransported ions behaves as an effector mechanism that could reflect a maximal density of ion channels or transporters.

3.3. Simplifying the "core" and the "shell": short-term cell volume regulation based on cotransport of ions sensing just cell volume

The complexity of the aforementioned models hindered analytical mathematical analysis. However, in a simpler model this could be achieved (Lucio et al., 2003). For this model, all the solute species were condensed into a single one and Eqs. (2) and (5) of Sections 3.2.1 and 3.2.2 are here replaced by:

$$\frac{dV}{dt} = P_{OSM} A V_W \left(\frac{m_s}{V} - C_{se}\right) \tag{11}$$

$$\frac{dm_s}{dt} = \alpha\left(\frac{V_R - V}{V_0}\right) \tag{12}$$

where C_{se} and m_s represent the extracellular concentration and the total number of moles of this lumped solute (denoted by subscript s), respectively. V_0 is the initial cell volume in the absence of any osmotic gradient, V_R is the cell volume after regulation is completed and α is a proportionality constant. These two parameters can be interpreted as the volume sensor and the effector mechanism, respectively. In this model the signalling process cannot be distinguished. Even though, if we think in terms of the time lag of the previous strategy (Section 3.2.4), we can consider that this model shows a time lag of zero. This means that the effector response would be instantaneous. This consideration is not consistent with previous fitting using the previous model to different vertebrate species in which time lags ranging from 17 to 34 min were observed (Espelt et al., 2008). However, this simplified model was successfully fitted to experimental cell volume kinetics of MDCK cells under RVI (Lucio et al., 2003).

3.4. Extracellular nucleotides in the signalling process of short-term cell volume regulation

In the previous models the signalling process was neglected or lumped into a single parameter τ, the time lag in the model of Hernandez and Cristina (1998). However, this is an *ad hoc* simplification since the signalling process involves complex pathways. As it was mentioned in the biological introduction of this section, nucleotides, mainly ATP, play the role of autocrine or paracrine signals in the RVD process (Wang et al., 1996). In the last ten years the dynamics of nucleotides in the extracellular space has been studied through mathematical modelling (for a review see Chara et al., 2011).

To model the dynamics of ATP in the extracellular space after a hypotonic shock the following general expression can be considered:

$$\frac{d[ATP]_e}{dt} = \sum_i J_i^{ATP,source} - \sum_j J_j^{ATP,sink} \tag{13}$$

where $J_i^{ATP,source}$ and $J_i^{ATP,sink}$ are the sources i and sinks j of extracellular ATP. The problem of modelling ATP in the extracellular space may be restricted to three main points: (1) to identify the nature of the sources and sinks, (2) to estimate the quantitative expressions which better describe them and (3) to estimate all the parameter values, validating the model using detailed quantitative data from experiments.

The sources of ATP in the extracellular medium can be further divided into non-lytic and lytic fluxes. The non-lytic release of ATP stems from biochemical machinery located at the plasma membrane. Due to the absence of direct experimental evidence, this process was modelled using empirical functions for A6 epithelia (Gheorghiu and Van Driessche, 2004) as well as for goldfish hepatocytes (Chara et al., 2009; Pafundo et al., 2008). Additionally, a mechanism involving simple diffusion was proposed for goldfish hepatocytes predicting the permeability values for ATP after fitting to experimental results which showed a good agreement with independent experimental information (Chara et al., 2010). Although ATP could be transported across a plethora of different biochemical machineries including CFTR, VSDAC, connexins, and pannexins, among others (Praetorius and Leipziger, 2009) the non-lytic flux is usually not sufficient to capture the experimental observations. During a hypotonic shock, a small number of cells could suffer membrane rupture. Since ATP concentration is in the order of micromolar in the intracellular compartment, the loss of membrane integrity could yield a lytic ATP flux. Only few mathematical models consider this lytic release of ATP based on accurate measurements of the number of cells suffering lysis (extracted from subsequent cell viability assays) and intracellular ATP concentration during the time course of hypotonic exposition (Chara et al., 2009, 2010; Pafundo et al., 2008). The diffusion of ATP in the extracellular space was modelled as a sink for A6 epithelia (Gheorghiu and Van Driessche, 2004), for retinal astrocytes and Mueller cells (Newman, 2001), and for goldfish hepatocytes (Chara et al., 2009; Pafundo et al., 2008). However, the most important sink in the extracellular space seems to be the ectonucleotidase activity, which has been modelled for blood vessels (Choi et al., 2007), airway epithelia (Zuo et al., 2008) and goldfish hepatocytes (Chara et al., 2009, 2010; Pafundo et al., 2008).

The considered cellular scale models depend on parameters for ion channel properties (P_J in Eqs. (5) and (6)), water channel properties (P_{OSM} in Eqs. (2), (4) and (11)) and cotransporter activities (α in Eq. (12)). In a tissue context these cellular properties will be subject to regulation due to cell–cell interactions, mechanical forces, signal concentrations, *etc.* which themselves are consequences of cellular behaviour. In Section 4 we will review tissue scale fluid transport and then discuss an example of cyst growth which illustrates the integration of aspects from different scales.

4. Tissue scale aspects

4.1. Fluid transport across epithelia

Cysts are tissues comprised of one or multiple bent epithelial cell layers that enclose a fluid-filled lumen. Solute accumulation

inside the lumen drives water influx into the cyst lumen and consequently leads to water accumulation and cyst expansion. A closed feedback loop of cyst growth and fluid transport results from stretch-induced cell divisions or stretch-dependent orientation of the cell division plane at the cellular scale (Shraiman, 2005). It is then an interesting question: which dependencies among tissue morphogenesis and fluid transport emerge at the tissue scale and would model cysts grow indefinitely? These questions have been addressed with the help of *in silico* models (Engelberg et al., 2011; Kim et al., 2009; Rejniak and Anderson, 2008; Grant et al., 2006) and mathematical analysis (Gin et al., 2010). Another question arises when signals are transmitted among the cells of the cyst by means of secreting ligands into the cyst lumen and sensing their concentration as observed for zebrafish mechanosensory organ formation (Durdu et al., 2014). In analogy to cell volume homeostasis as a guardian of signal transduction fidelity at the cell scale, lumen volume homeostasis is required as a guardian of signal transduction fidelity at the tissue scale. The question for a tissue model is: which mechanisms would be sufficient to let a cyst grow until a steady state and then show lumen volume homeostasis?

4.2. Model "cores" and "shells" at epithelial level

The model core, mechanisms of fluid production and the pathways followed by solutes and water across epithelia, can be seen as a parallel execution of single cell behaviour and hence be modelled in a similar manner. Additionally, properties not present at the single cell scale like bio-mechanic properties of the tissue have to be considered at the tissue scale. The epithelium shall not be modelled just as a passive structure allowing transport but also as a dynamical system responding to the changes in the solutions facing the layers. Although a respective model would need to be more complex, it would allow the study of epithelial systems at longer time or space scales. Here, the idea of modelling cores and shells discussed in Section 3 can be of advantage as well.

4.3. Models of fluid transport and tissue morphogenesis of cysts

In a series of studies, the *in silico* epithelial analogues ISEA I (Grant et al., 2006) and ISEA II (Kim et al., 2009) as well as an *in silico* MDCK analogue ISMA (Engelberg et al., 2011) have been developed as computational tools to analyse cystogenesis and have been validated for data from Madin-Darby canine kidney (MDCK) cell cysts. The ISEAs are agent-based, discrete models with up to twelve different rules that control the temporal update of individual cells and of the lumen size. Rules that add or remove lumen nodes correspond to the model core and the other rules represent the shell components that determine the cyst shape and thereby modulate the core components. Numerical simulations for different parameter choices have revealed the emergent behaviour of cystogenesis at the tissue scale as well as consequences of dysregulation which was modelled as parameter changes at the cell scale (Kim et al., 2009). The ISMA combines the rules of ISEA with spatially articulated cell shapes of the cellular Potts model for studying dynamic cell polarization during cystogenesis (Engelberg et al., 2011). Simulations showed the *de novo* generation of cysts from cell aggregates as well as their growth, in agreement with experimental data. Cyst growth slowed down and stopped for many investigated parameter settings. However, it is time-consuming to study the growth limits by means of simulations and it is impossible to draw conclusions for the entire high-dimensional parameter space. These problems become even more difficult for more detailed representations of cell dynamics, as in the immersed boundary cell model framework (Rejniak and Anderson, 2008).

To ease the study of growth limits and to derive as many of the computational rules as possible from biophysical mechanisms, a complementary continuum approach is useful. The model by Gin et al. (2010) provides such an approach and is here summarized in a simplified form with constant solute secretion flux I per cell into the cyst lumen. Their model can be understood in terms of a core *à la* Kedem–Katchalsky of local osmosis and solute secretion as well as a shell given by the elastic pressure and its relationship with cell density dynamics.

$$\frac{dV}{dt} = \chi A \Delta P \tag{14}$$

$$\frac{dC}{dt} = \frac{IN}{V} - \delta_C NC - \frac{C dV}{V dt} \tag{15}$$

$$\frac{dN}{dt} = rN - \delta_N N \tag{16}$$

$$\Delta P = \alpha(C - C_0) - \beta \Delta A \tag{17}$$

$$\Delta A = A - NA_1 \tag{18}$$

$$V = \gamma A \tag{19}$$

$$r = \frac{\kappa \Delta A}{NA_1} \tag{20}$$

This model describes water and solute transport (Eqs. (14) and (15) represent the model core) across the surface area A of a cyst's lumen constituted by N cyst cells (Eqs. (16)–(20) represent the model shell). The pressure difference ΔP constitutes the driving force for water transport across the cells which increases ($\Delta P > 0$) or decreases ($\Delta P < 0$) the cyst volume V. The parameter χ is proportional to the water permeability which reflects the activity of water channels or aquaporins. It is assumed that the pressure difference ΔP between the region outside the cyst and the lumen is given by two contributions (Eq. (17)): the osmotic pressure difference, proportional (where α is the product between the gas constant, R, and the absolute temperature, T) to the difference of total solutes' concentrations in the lumen (C) and outside the cyst (C_0), and the elastic pressure, proportional (where β is the ratio between the Young modulus, E, and the cyst surface area, A) to the surface area increase ΔA. In the model, the luminal solute concentration C is increased by the trans-cellular solute flux I, actively pumped by each cell, and decreased by a linear leak and by dilution (Eq. (15)). An increase of cyst volume stretches the apical area of each cell and the total cyst surface area by ΔA (Eq. (18)). For ease of calculations, the cyst volume and surface area are here chosen to be proportional (Eq. (19)) which specifies cyst shape as more tubular than spherical. Finally, in this model, it is assumed that the N cells proliferate with rate r and leave the cyst with rate δ_N (Eq. (16)). This leaving process could be composed of apoptosis and/or differentiation and migration out of the epithelium (epithelial–mesenchymal transition) depending on the specific biological context. The proliferation rate r is here considered as proportional to the cyst's relative degree of stretching and hence equal to $\kappa \Delta A/(NA_1)$, where A_1 is the unstretched apical area of a single cell and κ is the scale of the proliferation rate (Eq. (20)).

Analysis shows that the above model lets cysts expand and stretch on a short time scale and grow through cell proliferation on a long time scale (Gin et al., 2010). However, lumen growth is not unlimited in this model but approaches a stable steady state and hence shows lumen volume homeostasis. The steady state solution is here obtained as a closed-form expression and this was the reason to introduce and analyse the simplified cyst model in Eqs. (14)–(20):

$$N^* = \frac{1}{\gamma A_1 \left(1 + \frac{\delta_N}{\kappa}\right)} V^* \tag{21}$$

$$C^* = \frac{I}{\delta_C V^*} \frac{1}{} \tag{22}$$

$$V^* = aC_0 \left(\sqrt{1 + \frac{2I}{a\delta_C C_0^2}} - 1 \right) \tag{23}$$

$$\text{with} a = \frac{\alpha\gamma}{2\beta} \left(1 + \frac{\kappa}{\delta_N}\right) \tag{24}$$

Since water permeability (and hence the activity of water channels or aquaporins) determines the transient dynamics of fluid transport and cyst growth then it is expected that also the asymptotic state (N^*, C^*, V^*) is determined by the magnitude of water permeability. Counter-intuitively, this permeability, denoted by χ, does not affect the steady state solution and therewith cyst volume is identical for fast or slowly swelling cysts.

Given this independence from water permeability, we wondered whether cyst swelling could be an intrinsic property of the proliferating cell layer itself and independent of the solute flux as well. As the analysis of Eq. (23) for physiologically motivated parameter values shows, the cyst volume is found to depend approximately linearly on the solute flux I (Fig. 3a). This proportional dependence was also found through numerical simulation of the full time course in the original cyst model by (Gin et al., 2010). Gin et al., 2007, 2010 considered the solute pump strength I to be a function of luminal solute concentration and degree of cell stretching. The proportionality is expected to break down for larger (possibly non-physiological) parameter ranges as the non-linear solution (Eq. (23)) determines.

Another important regulator of cyst swelling is the solute concentration C_0 outside of the cyst. The predicted asymptotic cyst volume depends in a non-trivial way on C_0 (Eq. (23)). One could expect from Eq. (23) that cyst volume increases with increasing C_0 but as Fig. 3b shows, the inverse is true for physiologically

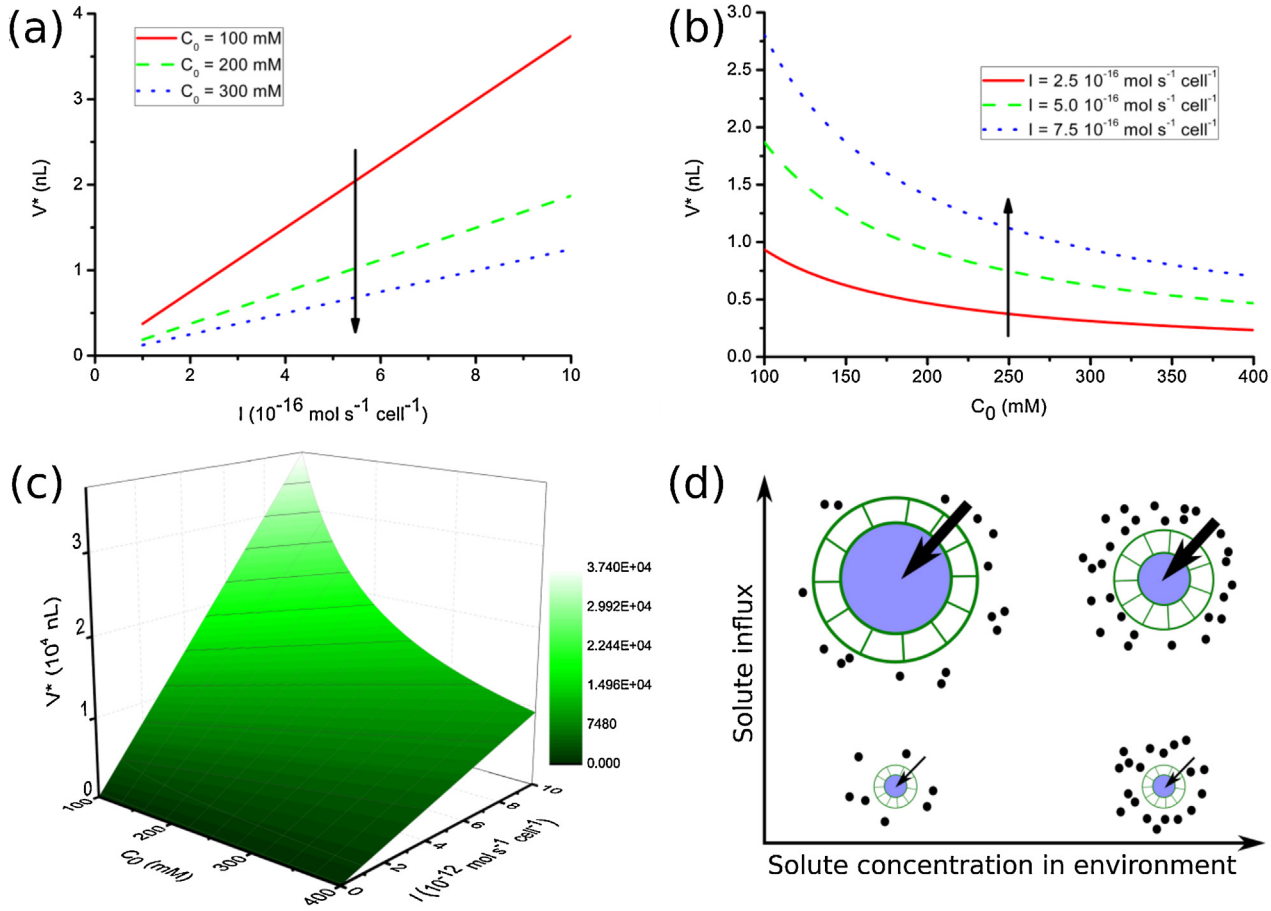

Fig. 3. Model of fluid transport into the lumen of a cyst. (a) Steady state lumen volume (V^*) as a function of the solute flux across each cyst cell (I) at three fixed values of the solute concentration outside of the cyst (C_0), from Eq. (23). (b) Steady state lumen volume (V^*) as a function of the solute concentration outside of the cyst (C_0) at three fixed values of the solute flux across each cyst cell (I), from Eq. (23). In (a) and (b) the arrow shows increasing C_0 and I, respectively. (c) 3D surface showing the steady state lumen volume (V^*) from the non-linear solution (Eq. (23)) as a function of the solute concentration outside of the cyst (C_0) and the solute flux across each cyst cell (I) for a larger range of I than in (a) and (b). (d) Qualitative overview of the effect of varying C_0 and I on the steady state lumen volume. The exact solution (Eq. (23)) is shown for $E = 4.37 \times 10^{-1}$ dyn cm^{-2}, $\delta_N = 2.67 \times 10^{-6}$ s^{-1}, $\delta_C = 2.67 \times 10^{-6}$ s^{-1}, $\kappa = 1.0$ s^{-1}, $A_1 = 3.14 \times 10^{-6}$ cm^2 and other parameters as estimated in (Cattoni and Chara, 2008).

motivated parameter values. In particular, the small $I \ll a\delta_C C_0^2$ lets us expand the root and find $V^* \approx \frac{I}{\delta_C C_0}$ which is numerically confirmed in Fig. 3c.

Altogether, increasing I or decreasing C_0 increase cyst volume and *vice versa* (Fig. 3d). Quantitatively, the model linking cellular aspects such as solute pump strength I with tissue scale aspects like cyst volume V allows to gain mechanistic understanding of otherwise counter-intuitive (*e.g.* V^* independent of water permeability and $V^*(C_0)$) and surprising (*e.g.* $V^*(I)$) dependencies.

5. Open biological questions

Zebrafish serves as a versatile model organism to study vertebrate development. The left–right axis of the embryo is established by fluid–cell interactions inside a tissue cyst, called Kupffer's vesicle (Compagnon et al., 2014; Oteíza et al., 2008). The lumen diameter grows up to 50 μm within about 100 min and it remains to be determined how such rapid growth is achieved and which solutes are responsible. Failure to expand the cyst lumen would render this laterality organ non-functional.

Luminal signalling by secreted FGF ligands within the micro-lumen of tissue rosettes has recently been quantified (Durdu et al., 2014). The rosettes of the zebrafish lateral line primordium eventually form mechanosensory organs. FGF ligand concentration inside the microlumen (diameter on the order of 5 μm) of each rosette controls organ location. Zebrafish possess a row of multiple organs with sequentially smaller spacing between them, in anterior-posterior order, presumably caused by sequentially higher luminal FGF concentration since stronger FGF signals trigger faster deposition at correspondingly shorter distance. Two hypothetical mechanisms for the increase of FGF concentrations can be considered: (1) FGF expression levels raise or (2) lumen volume shrinks in anterior-posterior order. The second hypothesis will be interesting to test experimentally. Compared to the reported artificial expression perturbations (Durdu et al., 2014), we expect as strong but inverse effects from perturbations of lumen volume which may depend on vesicular and/or osmotic fluid transport.

As presented in Section 4, cyst lumen expansion can saturate despite ongoing solute secretion because the driving force of the osmotic gradient is diluted and diminished as a result of its action. We now imagine to open up the cyst and ask how a sustained secretory fluid flux can be generated. This would entail solute efflux and the challenge of continuous solute secretion (Fischbarg, 2010; Shachar-Hill and Hill, 2002; Whittembury and Reuss, 1992; Reuss, 2008; Hill, 2008). Moreover, in the specific case of bile-secreting hepatocytes, each hepatocyte is not only subject to the osmotic gradient generated by its own bile salt secretion but also to the bile salts of all its upstream neighbour hepatocytes *via* the tissue-scale bile flow pattern. Again, we will need to consider regulatory feedback that links the tissue scale to the cell scale.

6. Conclusions

Fluid transport across barriers, such as membranes and epithelia, is crucial and tightly regulated. The regulatory mechanisms often span across multiple spatial scales from cellular interactions up to the architecture of organs. For understanding cell physiology better, modellers earlier had to shift their perspective from considering the cell as a mere 'bag of enzymes' (Cornish-Bowden and Cárdenas, 2000; Hogeboom et al., 1953) to considering the complex micro-architecture and compartmentalisation inside (Kupinski et al., 2013; Foret et al., 2012; Lauffenburger and Linderman, 1993). We have here asked " . . . but what about the 'bag' part?" and discussed models in which biochemistry has been combined with biophysics. We propose that fluid transport models at any scale can be constructed in a core–shell framework, in which the core accounts for the biophysical effects of fluid transport whilst the shell reflects the regulatory mechanisms. As experimental studies of fluid transport and related physiological processes at the tissue scale are extending to mechanistic and quantitative aspects, mathematical modelling will help us to integrate these tissue-scale aspects with regulatory mechanisms at the cellular as well as molecular scales and therefore understand even counter-intuitive observations. We expect that this multi-scale perspective on fluid transport will also be required to address open questions in the field of Systems Medicine.

Acknowledgements

We are grateful to Andreas Deutsch, Marcelo Ozu and Oleksandr Ostrenko for fruitful discussions and to Michelle Rother for help with generating figures. The authors acknowledge support by the Human Frontier Science Program (HFSP, grant RGP0016/2010) and by the German Ministry for Education and Research through the Virtual Liver Network (BMBF, grant 0315734). Osvaldo Chara is career researcher from Consejo Nacional de Investigaciones Científicas y Técnicas (CONICET) of Argentina.

References

Altamirano, J., Brodwick, M.S., Alvarez-Leefmans, F.J., 1998. Regulatory volume decrease and intracellular Ca^{2+} in murine neuroblastoma cells studied with fluorescent probes. J. Gen. Physiol. 112, 145–160.
Baumgarten, C.M., Feher, J.J., 1995. Cell Physiology Source Book. In: Sperelakis, N. (Ed.), Academic, New York, pp. 180–211.
Bedzhov, I., Zernicka-Goetz, M., 2014. Self-organizing properties of mouse pluripotent cells initiate morphogenesis upon implantation. Cell 156, 1032–1044.
Busse, F.H., Müller, S.C., 1998. Evolution of Spontaneous Structures in Dissipative Continuous Systems. Springer, Berlin, Heidelberg.
Byrne, J.H., Schultz, S.G., 1988. An Introduction to Membrane Transport and Bioelectricity. Raven Press, New York.
Cattoni, D.I., Chara, O., 2008. Vacuum effects over the closing of enterocutaneous fistulae: a mathematical modeling approach. Bull. Math. Biol. 70 (1), 281–296.
Chara, O., Espelt, M.V., Krumschnabel, G., Schwarzbaum, P.J., 2011. Regulatory volume decrease and P receptor signaling in fish cells: mechanisms, physiology, and modeling approaches. J. Exp. Zool. A 315 (4), 175–202.
Chara, O., Pafundo, D.E., Schwarzbaum, P.J., 2009. Kinetics of extracellular ATP from goldfish hepatocytes: a lesson from mathematical modeling. Bull. Math. Biol. 71, 1025–1047.
Chara, O., Pafundo, D.E., Schwarzbaum, P.J., 2010. Negative feedback of extracellular ADP on ATP release in goldfish hepatocytes: a theoretical study. J. Theor. Biol. 264, 1147–1158.
Choi, H.W., Ferrara, K.W., Barakat, A.I., 2007. Modulation of ATP/ADP concentration at the endothelial surface by shear stress: effect of flow recirculation. Ann. Biomed. Eng. 35, 505–516.
Compagnon, J., Barone, V., Rajshekar, S., Kottmeier, R., Pranjic-Ferscha, K., Behrndt, M., Heisenberg, C.-P., 2014. The notochord breaks bilateral symmetry by controlling cell shapes in the zebrafish laterality organ. Dev. Cell 31 (6), 774–783.
Cornish-Bowden, A., Cárdenas, M.L., 2000. Technological and Medical Implications of Metabolic Control Analysis Nato Science Partnership Subseries: 3, Vol. 74. Springer.
Durdu, S., Iskar, M., Revenu, C., Schieber, N., Kunze, A., Bork, P., Schwab, J.M., Gilmour, D., 2014. Luminal signalling links cell communication to tissue architecture during organogenesis. Nature 515 (7525), 120–124.
Eiraku, M., Takata, N., Ishibashi, H., Kawada, M., Sakakura, E., Okuda, S., Sekiguchi, K., Adachi, T., Sasai, Y., 2011. Self-organizing optic-cup morphogenesis in three-dimensional culture. Nature 472, 51–56.
Engelberg, J.A., Datta, A., Mostov, K.E., Hunt, C.A., 2011. MDCK cystogenesis driven by cell stabilization within computational analogues. PLoS Comput. Biol. 7 (4), e1002030.
Espelt, M.V., Alleva, K., Amodeo, G., Krumschnabel, G., Rossi, R.C., Schwarzbaum, P.J., 2008. Volumetric response of vertebrate hepatocytes challenged by osmotic gradients: a theoretical approach. *Comp. Biochem. Physiol. B Biochem. Mol. Biol.* 150, 103–111.
Ferrara, C.G., Chara, O., Grigera, J.R., 2012. Aggregation of non-polar solutes in water at different pressures and temperatures: the role of hydrophobic interaction. J. Chem. Phys. 137 (13), 135104.
Fischbarg, J., 2010. Fluid transport across leaky epithelia: central role of the tight junction and supporting role of aquaporins. Physiol. Rev. 90 (4), 1271–1290.
Ford, P., Rivarola, V., Chara, O., Blot-Chabaud, M., Cluzeaud, F., Farman, N., Parisi, M., Capurro, C., 2005. Volume regulation in cortical collecting duct cells: role of AQP2. Biol. Cell 97 (9), 687–697.

Foret, L., Dawson, J.E., Villaseñor, R., Collinet, C., Deutsch, A., Brusch, L., Zerial, M., Kalaidzidis, Y., Jülicher, F., 2012. A general theoretical framework to infer endosomal network dynamics from quantitative image analysis. Curr. Biol. 22 (15), 1381–1390.
Freitas Jr, R., 1999. Nanomedicine. Volume I: Basic Capabilities. Landes Bioscience.
Ganti, T., 2003. The Principles of Life. Oxford University Press.
Gheorghiu, M., Van Driessche, W., 2004. Modeling of basolateral ATP release induced by hypotonic treatment in A6 cells. Eur. Biophys. J. 33, 412–420.
Gin, E., Crampin, E.J., Brown, D.A., Shuttleworth, T.J., Yule, D.I., Sneyd, J., 2007. A mathematical model of fluid secretion from a parotid acinar cell. J. Theor. Biol. 248 (1), 64–80.
Gin, E., Tanaka, E.M., Brusch, L., 2010. A model for cyst lumen expansion and size regulation via fluid secretion. J. Theor. Biol. 264, 1077–1088.
Goldman, D.E., 1943. Potential, impedance, and rectification in membranes. J. Gen. Physiol. 27, 37–60.
Grant, M.R., Mostov, K.E., Tlsty, T.D., Hunt, C.A., 2006. Simulating properties of in vitro epithelial cell morphogenesis. PLoS Comput. Biol. 2 (10), e129.
Hallows, K.R., Knauf, P.A., 1994. Cellular and Molecular Physiology of Cell Volume Regulation. In: Strange, K. (Ed.), CRC, pp. 3–29.
Hernandez, J.A., Cristina, E., 1998. Modeling cell volume regulation in nonexcitable cells: the roles of the Na^+ pump and of cotransport systems. Am. J. Physiol. 275, C1067–C1080.
Hill, A.E., 2008. Fluid transport: a guide for the perplexed. J. Membr. Biol. 223 (1), 1–11.
Hodgkin, A.L., Katz, B., 1949. The effect of sodium ions on the electrical activity of the giant axon of the squid. J. Physiol. 108, 37–77.
Hoffmann, E.K., Lambert, I.H., Pedersen, S.F., 2009. Physiology of cell volume regulation in vertebrates. Physiol. Rev. 89 (1), 193–277.
Hogeboom, G.H., Schneider, W.C., Striebich, M.J., 1953. Localization and integration of cellular function. Cancer Res. 13 (9), 617–632.
Jakab, M., Furst, J., Gschwentner, M., Botta, G., Garavaglia, M.L., Bazzini, C., Rodighiero, S., Meyer, G., Eichmuller, S., Woll, E., Chwatal, S., Ritter, M., Paulmichl, M., 2002. Mechanisms sensing and modulating signals arising from cell swelling. Cell. Physiol. Biochem. 12, 235–258.
Kedem, O., Katchalsky, A., 1958. Thermodynamic analysis of the permeability of biological membranes to non-electrolytes. Biochim. Biophys. Acta 27 (2), 229–246.
Kim, S.H., Park, S., Mostov, K., Debnath, J., Hunt, C.A., 2009. Computational investigation of epithelial cell dynamic phenotype in vitro. Theor. Biol. Med. Model 6, 8.
Klipp, E., Nordlander, B., Krüger, R., Gennemark, P., Hohmann, S., 2005. Integrative model of the response of yeast to osmotic shock. Nat. Biotechnol. 23, 975–982.
Kubitz, R., Häussinger, D., 2007. Osmoregulation of bile formation. Methods Enzymol. 428, 313–324.
Kupinski, A.P., Raabe, I., Michel, M., Ail, D., Brusch, L., Weidemann, T., Bökel, C., 2013. Phosphorylation of the Smo tail is controlled by membrane localization and is dispensable for clustering. J. Cell Sci. 126, 4684–4697.
Lancaster, M.A., Renner, M., Martin, C.-A., Wenzel, D., Bicknell, L.S., Hurles, M.E., Homfray, T., Penninger, J.M., Jackson, A.P., Knoblich, J.A., 2013. Cerebral organoids model human brain development and microcephaly. Nature 501, 373–379.
Landau, L.D., Lifshitz, E.M., 1980. third ed. Statistical Physics, vol. 5. Butterworth-Heinemann.
Lang, F., Busch, G.L., Ritter, M., Volkl, H., Waldegger, S., Gulbins, E., Haussinger, D., 1998. Functional significance of cell volume regulatory mechanisms. Physiol. Rev. 78, 247–306.
Lauffenburger, D.A., Linderman, J.J., 1993. Receptors: Models for Binding, Trafficking, and Signaling. Oxford University Press, Inc., New York.
Lazarowski, E.R., Boucher, R.C., Harden, T.K., 2003. Mechanisms of release of nucleotides and integration of their action as P2X- and P2Y-receptor activating molecules. Mol. Pharmacol. 64, 785–795.
Lucio, A.D., Santos, R.A., Mesquita, O.N., 2003. Measurements and modeling of water transport and osmoregulation in a single kidney cell using optical tweezers and videomicroscopy. Phys. Rev. E 68, 041906.
MacKnight, A.D.C., 1987. Volume maintenance in isosmotic conditions. Curr. Top. Membr. Transp. 30, 3–43.
Maria, G., 2005. Modular-based modelling of protein synthesis regulation. Chem. Biochem. Eng. Q. 19 (3), 213–233.
Maria, G., 2014. Extended repression mechanisms in modelling bistable genetic switches of adjustable characteristics within a variable cell volume modelling framework. Chem. Biochem. Eng. Q. 28 (1), 35–51.
Mühlfeld, S., Domanova, O., Berlage, T., Stross, C., Helmer, A., Keitel, V., Häussinger, D., Kubitz, R., 2012. Short-term feedback regulation of bile salt uptake by bile salts in rodent liver. Hepatology 56 (6), 2387–2397.
Newman, E.A., 2001. Propagation of intercellular calcium waves in retinal astrocytes and Muller cells. J. Neurosci. 21, 2215–2223.
Novotny, J.A., Jakobsson, E., 1996. Computational studies of ion-water flux coupling in the airway epithelium. 2. Role of specific transport mechanisms. Am. J. Physiol. 270, C1764–C1772.
Oteíza, P., Köppen, M., Concha, M.L., Heisenberg, C.P., 2008. Origin and shaping of the laterality organ in zebrafish. Development 135 (16), 2807–2813.
Pafundo, D.E., Chara, O., Faillace, M.P., Krumschnabel, G., Schwarzbaum, P.J., 2008. Kinetics of ATP release and cell volume regulation of hyposmotically challenged goldfish hepatocytes. Am. J. Physiol. Regul. Integr. Comp. Physiol. 294, R220–R233.
Pickard, W.F., 2008. Modelling the swelling assay for aquaporin expression. J. Math. Biol. 57 (6), 883–903.
Praetorius, H.A., Leipziger, J., 2009. ATP release from non-excitable cells. Purinergic Signalling 5, 433–446.
Rejniak, K.A., Anderson, A.R., 2008. A computational study of the development of epithelial acini: I. Sufficient conditions for the formation of a hollow structure. Bull. Math. Biol. 70 (3), 677–712.
Reuss, L., 2008. Seldin and Giebisch's The Kidney: Physiology & Pathophysiology. In: Alpern, R.J., Hebert, S.C., Burlington, M.A. (Eds.), Elsevier Academic, pp. 147–168 ch. 5.
Sato, T., Clevers, H., 2013. Growing self-organizing mini-guts from a single intestinal stem cell: mechanism and applications. Science 340, 1190–1194.
Schaber, J., Klipp, E., 2008. Short-term volume and turgor regulation in yeast. Essays Biochem. 45, 147–160.
Shachar-Hill, B., Hill, A., 2002. Paracellular fluid transport by epithelia. Int. Rev. Cytol. 215, 319–350.
Shraiman, B.I., 2005. Mechanical feedback as a possible regulator of tissue growth. Proc. Natl. Acad. Sci. U. S. A. 102 (9), 3318–3323.
Strieter, J., Stephenson, J.L., Palmer, L.G., Weinstein, A.M., 1990. Volume-activated chloride permeability can mediate cell-volume regulation in a mathematical model of a tight epithelium. J. Gen. Physiol. 96, 319–344.
Terashima, K., Takeuchi, A., Sarai, N., Matsuoka, S., Shim, E.B., Leem, C.H., Noma, A., 2006. Modelling Cl^- homeostasis and volume regulation of the cardiac cell. Philos. Trans. A Math. Phys. Eng. Sci. 364, 1245–1265.
Wang, Y., Roman, R., Lidofsky, S.D., Fitz, J.G., 1996. Autocrine signaling through ATP release represents a novel mechanism for cell volume regulation. Proc. Natl. Acad. Sci. U. S. A. 93, 12020–12025.
Whittembury, G., Reuss, L., 1992. The Kidney: Physiology and Pathophysiology. In: Seldin, D.W., Giebisch, G. (Eds.), Raven, New York, pp. 317–360.
Zuo, P., Picher, M., Okada, S.F., Lazarowski, E.R., Button, B., Boucher, R.C., Elston, T.C., 2008. Mathematical model of nucleotide regulation on airway epithelia – implications for airway homeostasis. J. Biol. Chem. 283, 26805–26819.